Cell Elasticity-based Microfluidic Label-free Isolation of Metastatic Tumor Cells

Muhymin Islam[1,2,3], Waseem Asghar[1,2,3,6], Young-tae Kim[3,4] and Samir M. Iqbal[1,2,3,4,5*]

[1]*Nano-Bio Lab, University of Texas at Arlington, Arlington, TX 76019, USA.*
[2]*Department of Electrical Engineering, University of Texas at Arlington, Arlington, TX 76011, USA.*
[3]*Nanotechnology Research Center, Shimadzu Institute for Research Technologies, University of Texas at Arlington, Arlington, TX 76019, USA.*
[4]*Department of Bioengineering, University of Texas at Arlington, Arlington, TX 76010, USA.*
[5]*Joint Graduate Committee of Bioengineering Program, University of Texas at Arlington and University of Texas Southwestern Medical Center at Dallas, University of Texas at Arlington, Arlington, TX 76019, USA.*
[6]*Harvard-MIT Division of Health Sciences and Technology, Harvard Medical School, Boston, Massachusetts, USA.*

Authors' contributions

Authors MI and SMI designed the study. Authors MI and WA wrote the protocols. Authors MI and YTK performed experiments and statistical analysis. Author SMI supervised this work. All authors have read and approved the final manuscript.

Original Research Article

ABSTRACT

Aims: Circulating tumor cells (CTCs) have significant diagnostic value for cancer patients. We report a label-free, simple and rapid microchannel filter type device for isolation of known metastatic cancer cells based on their mechano-physical properties like size and deformability.
Study Design: Metastatic renal cancer cells were highly elastic and squeezed through microchannels much smaller than their size. Using a reverse-selectivity approach, the number of microchannels and their dimensions were varied to optimize and reduce the shear stress on tumor cells such that these did not pass through filtering channels.
Place and Duration of Study: Department of Electrical Engineering and Department of

---

*Corresponding author: Email: smiqbal@uta.edu;

Bioengineering, University of Texas at Arlington, USA, between June 2012 and March 2013.

Methodology: A microfluidic filter type device was fabricated using soft lithography in polydimethylsiloxane (PDMS). The device consisted of one inlet and one outlet connected via 400 microchannels. First of all human derived renal cancer cells were suspended in 1X PBS solution and passed through these microchannels and capture efficiency of the device was calculated. The dimensions of microchannels were varied in order to increase efficiency. Eventually cancer cells were spiked in rat blood and isolated from the mixture.

Results: For different dimensions of microchannels capture efficiencies of the devices were calculated. First device consisted of microchannels of 20 μm x 10 μm (Device-1) and the capture efficiency was 31.04±2.5%. Then dimensions were varied to 10 μm x 10 μm (Device-2), 10 μm x 5 μm (Device-3), and 5 μm x 5 μm (Device-4) and capture efficiencies increased to 45.18±1.85%, 70.96±2.39% and 78.36±4.29%, respectively. Rat blood was used as negative control in Device-3 and Device-4 and blood cells were able to pass the microchannels. Finally renal cancer cells were spiked in rat blood and isolated from red blood cells and white blood cells.

Conclusion: A novel microdevice is fabricated to detect metastatic renal cancer cells based on their size and deformability. The efficiency of the device is more than 78%. This microfluidic channel device does not require preprocessing of blood (except dilution) or tagging/modification of cells and can be implemented for primary screening of cancer.

1. INTRODUCTION

Circulating tumor cells separate from the solid tumor and circulate through blood to form secondary tumors [1]. CTCs are found in the blood for most of the cancer patients. It is important to detect CTCs in peripheral blood of cancer patients at early stages to prevent metastasis [1]. In 2012, a total of 1,638,910 new cancer cases and 577,190 deaths from cancer were projected to occur in the United States alone [2]. This is because early stage cancer is mostly asymptomatic and cannot be detected for effective treatment. Numerous conventional cancer cell sorting techniques including centrifugation, chromatography, and fluorescence-/magnetic-activated cell sorting (FACS and MACS) are limited in yield and purity [3]. Consequently, microfluidic systems have emerged as fascinating platforms to detect cancer cells. In recent years, magnetism based cell sorting, on-chip dielectrophoresis, functionalized and/or label-free microfluidic systems are getting considerable interest to detect cancer cells from simple body fluids.

Magnetic bead based cell separation techniques have been shown to isolate and enumerate CTCs from blood samples with high efficiency, specificity and viability [4-8]. In order to take the advantage of both immunomagnetic assay and the microfluidic device, immunomagnetic CTC detection has also been reported. Cancer cells have been labeled with magnetic nanoparticles and separated from blood flow using arrays of magnets [9]. Another microfluidic device has been shown to detect and culture CTCs collected from whole blood using EpCAM coated magnetic microbeads [10]. Dielectric properties of metastatic cancer cells are also known to be significantly different from normal blood cells and therefore dielectrophoresis (DEP) has been used to successfully detect CTCs with high efficiency and purity [11-19]. Numerous DEP techniques such as positive DEP, negative DEP, field flow

fractionation DEP, multi-orifice flow fractionation DEP [16], contactless DEP [18], etc. have been reported. But complexity (in design and/or operation), time consuming pre-processing and requirement of external magnetic or electric fields etc. are limiting factors in these techniques [20].

Due to high specificity and selectivity, aptamers have been incorporated in several microfluidic setups to detect and enrich tumor cells [21-24]. However aptamers are not available for all types of cancer biomarkers and their reproducible and faithful attachment to device surfaces is a long and tedious process. Therefore label-free microfluidic isolation that does not require multiple additional "tags" or "labels" of rare cells is preferable [20]. Distinctive physical properties of CTCs such as density, adhesion, size, and deformability can be used for label-free separation. Usually sizes of tumor cells are not only larger than red blood cells (RBCs) and white blood cells (WBCs) but also have higher elasticity [25]. Some metastatic cancer cell types have been reported to be more than 70% softer than benign cells and mechanical analysis can distinguish these from normal cells of similar shapes [26]. Some devices like microcavity array [27], small capillaries [28,29], 3D filters [30], pool-dam structures [31] and adhesion based nanostructured surfaces [32] use mechanical properties as discriminator of cancer cells from blood. On the other hand, some devices have employed structures like double spiral channels [33], multiple channel segments devices [34], parylene membranes [35,36] and herringbone-texturing [37]. Most efficient and commonly used label-free cell separation can be just filtration, based on size and deformability of cells. For cell sorting and fractionation, numerous microfilters are validated which can be categorized in 4 types namely weir, pillar, cross-flow and membrane [20].

Here we introduce a microfluidic filter type device that blocked cancer cells in spite of their highly elastic nature. The device consisted of single inlet and outlet chambers connected by 400 microchannels. The dimensions of the microchannels were optimized to block more than 78% of renal cancer cells in the inlet. This label-free, cost-effective and high-throughput approach could be implemented for rapid cell sorting based on their distinctive physical properties such as size and deformability without any pre-processing. Devices were fabricated in polydimethylsiloxane (PDMS) using soft-lithography with different cross-sectional areas of the channels by varying the width and height. The four types of devices with channel dimensions of 20 μm x 10 μm (Device-1), 10 μm x 10 μm (Device-2), 10 μm x 5 μm (Device-3) and 5 μm x 5 μm (Device-4) were fabricated. For every device here, dimension is represented as height x width. Blocking efficiency of these four devices for renal cancer cells were found to be 31.04%, 45.18%, 70.96% and 78.36% respectively. The smaller cross-sectional area increased the overall cell isolation efficiency showing specific behavior of RBCs and WBCs in these devices. It was observed from experiments that RBCs and WBCs were small enough to pass easily through the microchannels in Device-3 and Device-4. Eventually cancer cells were mixed with rat blood and Device-4 was able to detect tumor cells successfully.

2. EXPERIMENTAL DETAILS

All the chemicals were purchased from Sigma-Aldrich (St. Louis, MO) unless mentioned otherwise.

2.1 Microdevice Design and Fabrication

Dimensions of the microchannels were chosen based on cell sizes. The diameters of cancer cells have been reported to range between 11 µm to 22.5 µm [27], thus the experiments were started with channel dimensions of 10 µm x 20 µm. Several articles have suggested similar dimensions of channels to capture cancer cells [27-37]. It was reported elsewhere that WBCs and RBCs could traverse through 2-5 µm capillaries while cancer cells were captured [28]. Again, from simple mechanophysical analysis using Young's law it was calculated that for a specific flow rate of 1 ml/h, the final size of CTCs in a channel of dimension 10 x 20 µm^2 could be reduced to 9.99 µm and 19.99 µm for their initial diameter of 10 µm and 20 µm respectively. The Young's law describes a relationship among Young's modulus *Y*, applied pressure *P*, initial length *L* and change of length *l* of a substance by the following equation,

$$Y = P/(l/L) \tag{1}$$

For this calculation the Young's modulus of cancer cells was chosen as 0.5 kPa [26]. Therefore, it was expected to capture a good number of tumor cells using this device. But capture efficiency for this device was low and consequently the dimensions of the channels were reduced to enhance efficiency.

The dimensions of the inlet and outlet were 28 mm by 7 mm. The width of the microchannels was varied from 5 to 10 µm. First of all, the photo-masks were drawn in AutoCAD and patterns were produced on glass. The inlet and outlet were fabricated by spin coating SU-8 2010 on a silicon wafer (1000 rpm, 30 s). The height of the inlet and outlet was 22 µm. Next, the microchannels were fabricated using 10 µm high SU-8 2010 (spin coated at 1000 rpm for 30 s) and 5 µm height using SU-85 (spin coated at 3000 rpm for 30 s). The patterns were generated in masters using photolithography.

Next, the patterns were translated to PDMS. First of all, PDMS was mixed (10:1, wt/wt) with Sylgard 184 silicone elastomer curing agent (Dow Corning, Midland, MI). This mixture was degassed in a desiccator for 1 h to get rid of the bubbles. Then PDMS was poured on the masters and heated at 75 ºC for 5 min and then 150 ºC for 10 min. Next the PDMS molds were peeled off from the masters and fluidic ports were punched in every PDMS mold. These molds were cleaned in isopropyl alcohol (IPA), rinsed in de-ionized water (DI water) and dried in nitrogen. To cover PDMS, glass slides were used. The glass slides (50 mm x 75 mm) were already cleaned with piranha solution (H_2O_2:H_2SO_4 in a 1:3 ratio) for 10 min, rinsed with DI water and dried in nitrogen flow. The PDMS and glass slides were treated with UV Ozone plasma for 25 min and hermetically bonded together. Eventually the devices were filled with 1X PBS with 5 mM magnesium chloride (pH 7.5) to make these hydrophilic.

2.2 Cell Culture

Clear cell metastatic renal cell carcinoma samples were isolated from the brain tissues of consenting patient at the University of Texas Southwestern Medical Center at Dallas, Texas, USA as per the approved Institutional Review Board protocol [38]. The known metastasized renal derived cancer cells were collected in ice-cold Hank's medium. The cells were chemically dissociated with papain and dispase (both 2%) as reported earlier [39]. Next cells were cultured in Dulbecco's modified Eagle's medium (DMEM) with 10% fetal bovine serum [1]. The renal cancer cells were stably transduced with a lentivirus expressing mCherry

fluorescent protein. The blood samples were collected from tail of a rat by restraining the animal. The blood was collected in tubes with K2-EDTA as anticoagulant.

2.3 Experimental Setup and Procedure

The renal cancer cells were suspended in 1X PBS solution to desired concentrations. The cells were passed through the microfluidic channel device at flow rate of 1 ml/hr using a syringe pump. Although, higher flow rates would have reduced the processing time, the larger shear forces on the cells would have modified the cell behavior and selective filtration capability would have been lost. Cells were passed for 30 min and in order to avoid cell sedimentation the syringe was shaken after every 10 min. After passing the cells for 30 min, devices were scanned thoroughly and images were taken using optical microscope. The images were taken not only from channel areas, the whole device was observed to count cells. In addition, the cell solution that was coming out from the outlet chamber was collected and images were also taken of that solution to count the number of cells in the outlet. All of these images were analyzed to determine cell capture efficiency and to measure cell sizes using *ImageJ* software. In order to calculate cell capture efficiency, average number of cells passed to the outlet chamber and average number of cells captured in inlet chamber in per unit area were considered.

The cell viability was measured using the solution that was collected from outlet chamber. This solution was mixed with equal volume of trypan blue solution (0.4%) and was let sit for 5 min at room temperature. This solution was put on a glass slide and observed in optical microscope to count live and dead cells.

The blood samples were passed through devices after diluting with sterile 1X PBS at 1:10 ratio in order to reduce the sample viscosity [1]. Next, cancer cells were mixed in diluted blood at a concentration of 1000 cells/ml and this solution was used to run experiment in Device-4. After running experiments, the devices were observed in fluorescence microscope and images of the devices were taken. These images were analyzed using *ImageJ* software using same procedure mentioned above for calculating cell capture efficiency. The flow rate was kept moderate. In order to increase throughput, several devices can be used in parallel. Besides, number of channels can also be increased in each device, which could have allowed higher flow rate.

3. RESULTS AND DISCUSSION

3.1 Device Optimization and Calculation of Capture Efficiency

The microdevice design schematic is shown in Fig. 1. In order to define a baseline for cancer cell detection efficiency, high concentration of cancer cells were spiked in 1X PBS and pumped through the microdevices. Though the average diameter of renal cancer cells was more than 15 µm, most of the cells squeezed through the channels in Device-1 due to their highly elastic nature. But some cells were captured in the channels and cluster of cells were observed around the channels as shown in Fig. 2(a). The average capture efficiency (η) for this device was 31.04±2.5%, calculated using the following equation.

$$\eta = \frac{X}{X+Y} \times 100\%$$

(2)

Here variables X and Y represent the number of cells remaining in the inlet and the number of cells that made it to the outlet, respectively.
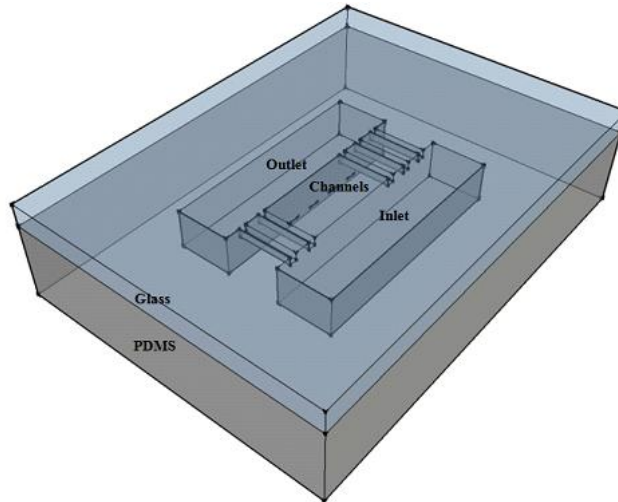

Fig. 1. Schematic diagram of the microfluidic channel device (flipped upside down)

There can be a number of plausible explanations to understand the passage of cells through the channels in addition to their mechanophysical properties. One factor could be the heterogeneity in the sizes of cancer cells. Another could be the shape of cells; cells are globular in shape whereas channels were rectangular and exact range of Young's moduli of cancer cell was unknown. But all these factors were unchanged from device to device, so their contributions can be discounted. To increase capture efficiency, the height was lowered to 10 μm (Device-2). The reduction in the total cross-sectional area available for the cells to pass through resulted in the increment of capture efficiency to 45.18±1.85%. Still, more than half of the cells were able to pass through the channels as shown in (Fig. 2b). Next, Device-3 and Device-4 showed capture efficiencies jumping to 70.96±2.39% and 78.36±4.29%, respectively (Fig. 2c, 2d and Fig. 3). Every device was run for two times and the results clearly exhibited a statistically different behavior that followed an almost monotonic trend. From Fig. 2, it can be observed that cells were passing through the channels in Device-1 and Device-2. Therefore the cell clusters were found on both sides of the channels (Fig. 2a and 2b). On the other hand, no clusters of cells were observed on the outlet side of the Device-3 and Device-4 (Fig. 2c and 2d). Moreover, as cells had more space to traverse through in Device-1 and Device-2 compared to Device-3 and Device-4, therefore more cells were found around the channels in first two devices.

It was also observed that all the cells were not of same size and sizes of the cells had significant impact on capture efficiency. From the analysis of the sizes of 100 randomly selected cells in each device, it was seen that the cells blocked in Device-1 had average diameters of 18.44±3.60 μm, while average diameter of the cells captured in Device-4 was 15.22±3.54 μm (Fig. 4). For Device-2 and Device-3 these diameters were 17.25±2.13 μm and 15.26±4.97 μm, respectively. From this analysis, it was seen that all cancer cells were not of same size and when these cells were pushed through a microchannel, they squeezed up to a certain limit depending on their sizes. This brings out an important aspect that cell elasticity depends on its size. Previous reports have just looked at elasticity of tumor cells

as a whole but maybe the elasticity is further dependent on the grade of tumorigenesis, stage of cell division, and amount of overexpression/downregulation of various markers.
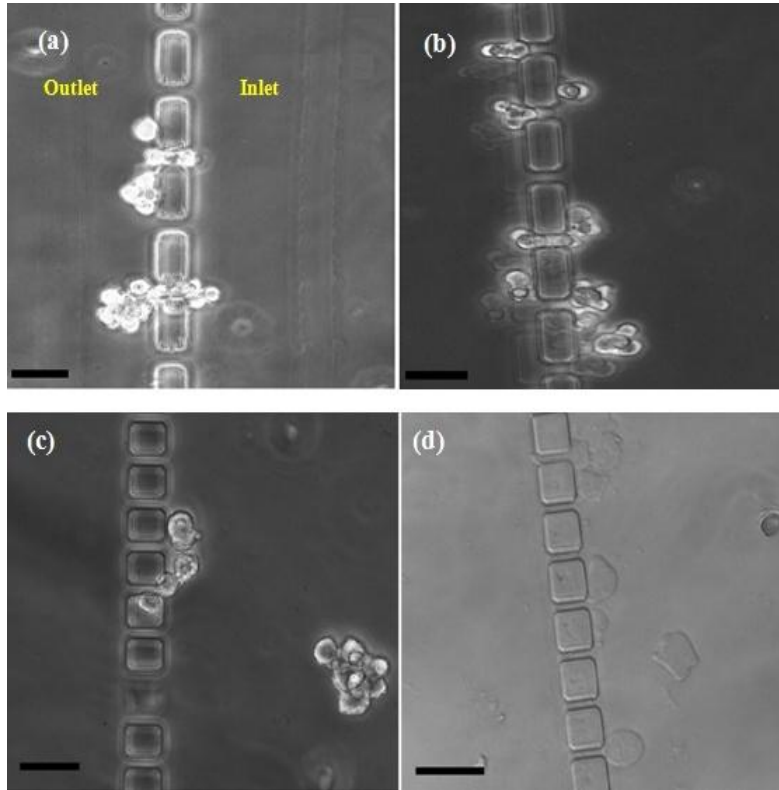

Fig. 2. Cells captured in microfluidic devices in case of (a) Device-1, (b) Device-2, (c) Device-3, and (d) Device-4. The scale bars in all micrographs are 50 µm. The right side of channels is inlet and the left is outlet as mentioned for (a).
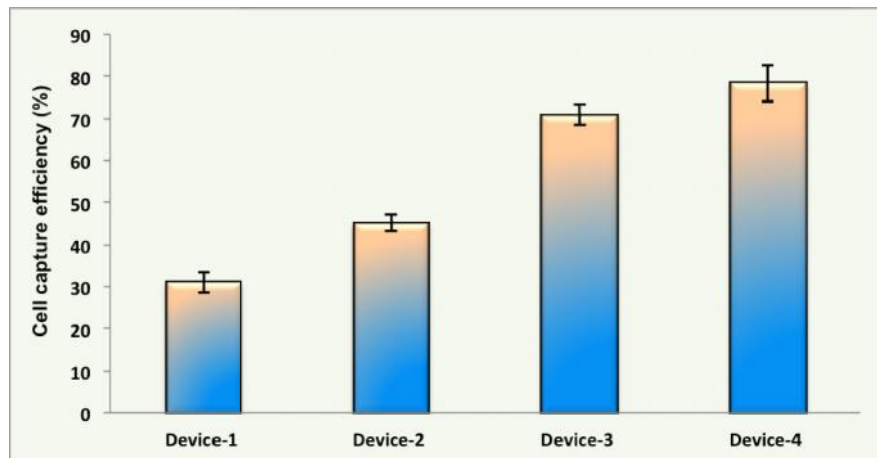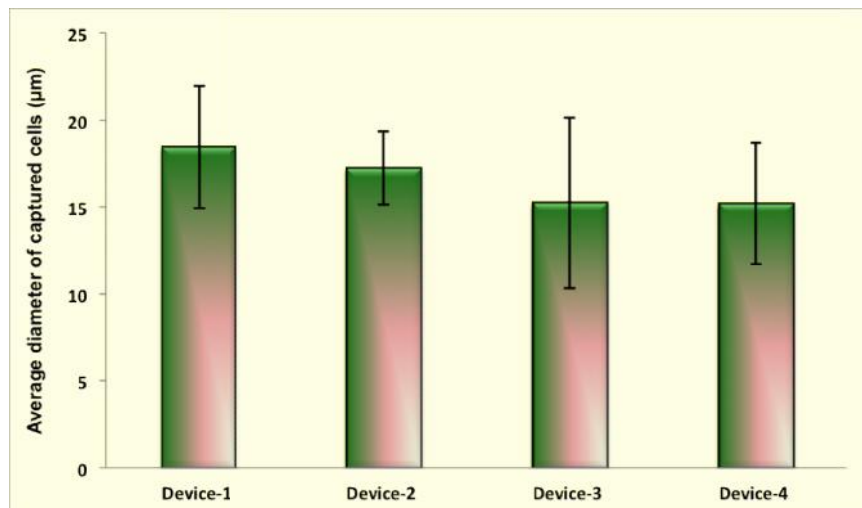

Fig. 3. Average cell capture efficiency of four devices (*n*=2).

Fig. 4. Average sizes of the blocked cells in four devices (*n*=100 for each).

As the flow rate was same for all cells, the pressure applied to each cell, and consequently the shear force, was also same. So if we consider all cells to have same Young's modulus then strain on each cell should also be the same. From the simple definition of Young's modulus final size of the cells should be linear function of their initial size. Consequently, larger cells were blocked and smaller cells passed through. In Device-4, viability of renal cancer cells was above 74%.

3.2 Detection of Cancer Cells from Blood

Diluted rat blood samples were used to run experiments in optimized devices (Device-3 and Device-4). It was observed that RBCs and WBCs were smaller in size and were able to pass the microchannels quite easily (Fig. 5). In Device-4, some WBCs were hindered by the microchannels but were able to pass the channels without creating any cluster or blockage. Though some WBCs may be larger in size but it has been reported before that RBCs and WBCs can traverse through capillaries of 2-5 µm [28]. The tumor cells were spiked in diluted blood at a concentration of 1000 cells/ml and experiment was run in Device-4.

From optical micrographs, it was observed that some cells were blocked by the channels. As WBCs and RBCs were able to traverse through the channels (Fig. 5b) and channel dimensions of Device-4 were optimized to capture renal cancer cells with high efficiency (Fig. 3), it might be safely concluded that the blocked cells from blood sample were indeed cancer cells. But for clear discrimination of tumor cells from blood cells and to calculate capture efficiency, fluorescent images of the devices were taken (Fig. 6). After analyzing all the images it was found that this device was able to isolate these tumor cells from blood mixture with an average efficiency of 78.20±2.57%.This was very similar to the efficiency that was achieved from the devices to isolate CTCs from PBS solution.
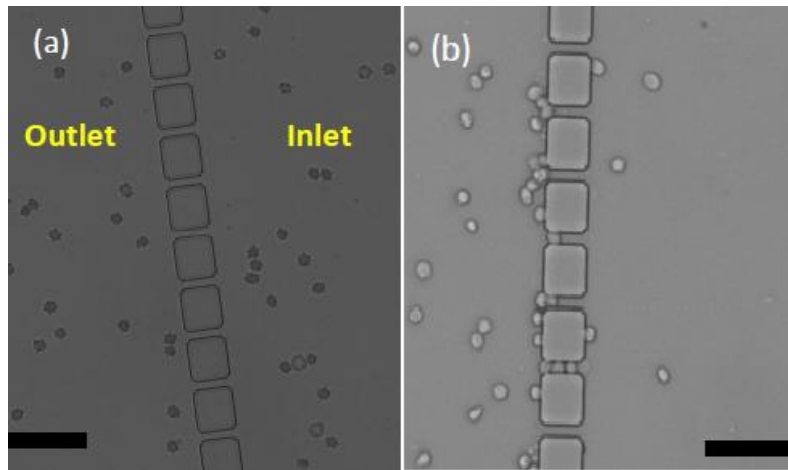
Fig. 5. Blood samples introduced in (a) Device-3, and (b) Device-4. RBCs and WBCs passed through the microchannels. The scale bars are 50 µm

It was also observed that tumor cells were very flexible and could change their shapes while trying to squeeze through the smaller channels, but clearly the shear force of the flow was not high enough. Smaller shear force did not result in the cell squeezing through, counter-intuitive to the more flexible nature of the cells. Some of the cells, captured by microchannels, were distorted in shapes.
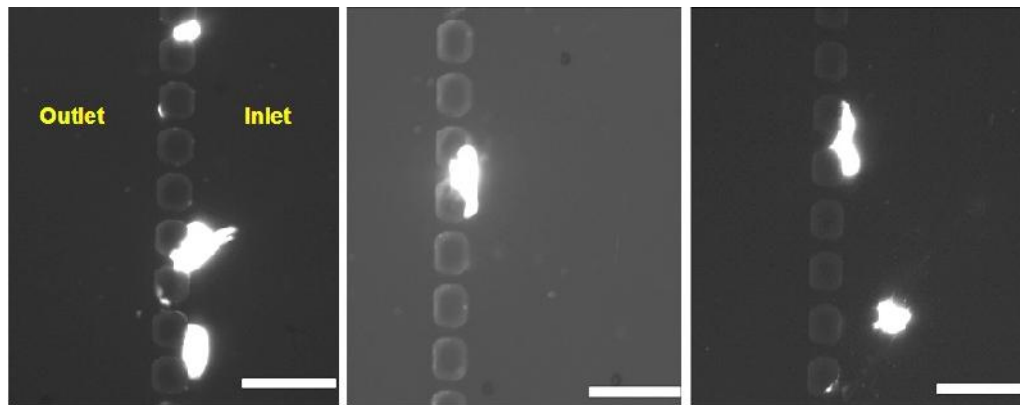

Fig. 6. Fluorescence micrographs of isolated cancer cells, spiked in rat blood, using Device-4. The scale bars are 50 µm.

4. CONCLUSION

A microdevice is shown to detect renal cancer cells, which were established already to be metastatic, based on their size and elasticity differences from RBCs and WBCs. Cancer cells are highly deformable and can squeeze through very small pores. The device consisted large number of channels to reduce shear stress on each cell which minimized the deformation of cancer cells and eventually detected renal cancer cells successfully with an efficiency of more than 78%. It was observed that the optimized channels were large enough

for WBCs and RBCs to pass through but reduced the shear force and plugging effect to capture metastatic tumor cells. This inexpensive and simple device can be used in CTC detection from blood samples.

CONSENT

The renal cancer cells were obtained from consenting patient after written informed consent as per the approved Institutional Review Board (IRB) protocol at the University of Texas Southwestern Medical Center at Dallas by our collaborator. These cells were gift to us for the experiments without revealing the identity of the patient.

ETHICAL APPROVAL

"All authors hereby declare that "Principles of laboratory animal care" (NIH publication No. 85-23, revised 1985) were followed, as well as specific national laws where applicable. All experiments have been examined and approved by the appropriate ethics committee"."All authors hereby declare that all experiments have been examined and approved by the appropriate ethics committee and have therefore been performed in accordance with the ethical standards laid down in the 1964 Declaration of Helsinki."

ACKNOWLEDGEMENTS

COMPETING INTERESTS

Authors have declared that no competing interests exist.

REFERENCES

1. Asghar W, et al. Electrical fingerprinting, 3D profiling and detection of tumor cells with solid-state micropores. Lab on a Chip. 2012;12(13):2345-2352.
2. Siegel R, Naishadham D, Jemal A. Cancer statistics. CA: A Cancer Journal for Clinicians. 2012;62:10-29.
3. Yu M, Stott S, Toner M, Maheswaran S, Haber DA. Circulating tumor cells: approaches to isolation and characterization. The Journal of Cell Biology. 2011;192(3):373-382.
4. Estes MD, Ouyang B, Ho S, Ahn CH. Isolation of prostate cancer cell subpopulations of functional interest by use of an on-chip magnetic bead-based cell separator. Journal of Micromechanics and Microengineering. 2009;19(9):095015-095022.
5. Saliba AE, et al. Microfluidic sorting and multimodal typing of cancer cells in self-assembled magnetic arrays. Proceedings of the National Academy of Sciences. 2010;107(33):14524-14529.
6. Sivagnanam V, Song B, Vandevyver C, Bünzli JCG, Gijs MAM. Selective breast cancer cell capture, culture, and immunocytochemical analysis using self-assembled magnetic bead patterns in a microfluidic chip. Langmuir. 2010;26(9):6091-6096.

7. Zhang K, et al. A microfluidic system with surface modified piezoelectric sensor for trapping and detection of cancer cells. Biosensors and Bioelectronics. 2010;26(2):935-939.
8. Chen CL, et al. Separation and detection of rare cells in a microfluidic disk via negative selection. Lab on a Chip. 2010;11(3):474-483.
9. Hoshino K, et al. Microchip-based immunomagnetic detection of circulating tumor cells. Lab on a Chip, 2011;11(20):3449-3457.
10. Kang JH, et al. A combined micromagnetic-microfluidic device for rapid capture and culture of rare circulating tumor cells. Lab on a Chip. 2012;12:2175-2181.
11. Becker FF, et al. Separation of human breast cancer cells from blood by differential dielectric affinity. Proceedings of the National Academy of Sciences. 1995;92(3):860-864.
12. Gascoyne PRC, Wang XB, Huang Y, Becker FF. Dielectrophoretic separation of cancer cells from blood. IEEE Transactions on Industry Applications. 1997;33(3):670-678.
13. Cheng J, Sheldon EL, Wu L, Heller MJ, O'Connell JP. Isolation of cultured cervical carcinoma cells mixed with peripheral blood cells on a bioelectronic chip. Analytical Chemistry. 1998;70(11):2321-2326.
14. Huang Y, Yang J, Wang XB, Becker FF, Gascoyne PRC. The removal of human breast cancer cells from hematopoietic CD34+ stem cells by dielectrophoretic field-flow-fractionation. Journal of Hematotherapy & Stem Cell Research. 1999;8(5):481-490.
15. Yang J, Huang Y, Wang XB, Becker FF, Gascoyne PRC. Cell separation on microfabricated electrodes using dielectrophoretic/gravitational field-flow fractionation. Analytical Chemistry. 1999;71(5):911-918.
16. Moon HS, et al. Continuous separation of breast cancer cells from blood samples using multi-orifice flow fractionation (MOFF) and dielectrophoresis (DEP). Lab on a Chip. 2008;11(6):1118-1125.
17. Gascoyne PRC, Noshari J, Anderson TJ, & Becker FF. Isolation of rare cells from cell mixtures by dielectrophoresis. Electrophoresis. 2009;30(8):1388-1398.
18. Gencoglu A, Minerick A. Chemical and morphological changes on platinum microelectrode surfaces in AC and DC fields with biological buffer solutions. Lab on a Chip. 2009;9(13):1866-1873.
19. Salmanzadeh A, et al. Isolation of prostate tumor initiating cells (TICs) through their dielectrophoretic signature. Lab on a Chip. 2012,12:182-189.
20. Gossett DR, et al. Label-free cell separation and sorting in microfluidic systems. Analytical and Bioanalytical Chemistry. 2010;397(8):3249-3267.
21. Nagrath S, et al. Isolation of rare circulating tumour cells in cancer patients by microchip technology. Nature. 2007;450(7173):1235-1239.
22. Adams AA, et al. Highly efficient circulating tumor cell isolation from whole blood and label-free enumeration using polymer-based microfluidics with an integrated conductivity sensor. Journal of the American Chemical Society. 2008;130(27):8633-8641.
23. Xu Y, et al. Aptamer-based microfluidic device for enrichment, sorting, and detection of multiple cancer cells. Analytical Chemistry. 2009;81(17):7436-7442.
24. Dharmasiri U, et al. Highly efficient capture and enumeration of low abundance prostate cancer cells using prostate-specific membrane antigen aptamers immobilized to a polymeric microfluidic device. Electrophoresis. 2009;30(18):3289-3300.
25. Lekka M, et al. Elasticity of normal and cancerous human bladder cells studied by scanning force microscopy. European Biophysics Journal. 1999;28(4):312-316.

26. Cross SE, Jin YS, Rao J, Gimzewski JK. Nanomechanical analysis of cells from cancer patients. Nature Nanotechnology. 2007;2(12):780-783.
27. Hosokawa M, et al. Size-selective microcavity array for rapid and efficient detection of circulating tumor cells. Analytical Chemistry. 2010;82(15):6629-6635.
28. Tan SJ, Yobas L, Lee GYH, Ong CN, Lim CT. Microdevice for the isolation and enumeration of cancer cells from blood. Biomedical Microdevices. 2009;11(4):883-892.
29. Tan SJ, et al. Versatile label free biochip for the detection of circulating tumor cells from peripheral blood in cancer patients. Biosensors and Bioelectronics. 2010;26(4):1701-1705.
30. Zheng S, et al. 3D microfilter device for viable circulating tumor cell (CTC) enrichment from blood. Biomedical Microdevices. 2011;13(1):203-213.
31. Chen Z, et al. Pool-dam structure based microfluidic devices for filtering tumor cells from blood mixtures. Surface and Interface Analysis. 2006;38(6):996-1003.
32. Kwon KW, et al. Label-free, microfluidic separation and enrichment of human breast cancer cells by adhesion difference. Lab on a Chip. 2007;7(11):1461-1468.
33. Sun J, et al. Double spiral microchannel for label-free tumor cell separation and enrichment. Lab on a Chip. 2012;12:3952-3960.
34. Mohamed H, et al. Development of a rare cell fractionation device: application for cancer detection. IEEE Transactions on Nano Bioscience. 2004;3(4):251-256.
35. Lin HK, et al. Portable filter-based microdevice for detection and characterization of circulating tumor cells. Clinical Cancer Research. 2010;16(20):5011-5018.
36. Xu T, Lu B, Tai YC, Goldkorn A. A cancer detection platform which measures telomerase activity from live circulating tumor cells captured on a microfilter. Cancer Research. 2010;70(16):6420-6426.
37. Stott SL, et al. Isolation of circulating tumor cells using a microvortex-generating herringbone-chip. Proceedings of the National Academy of Sciences. 2010;107(43):18392-18397.
38. Marin-Valencial, et al. Glucose metabolism via the pentose phosphate pathway, glycolysis and Krebs cycle in an orthotopic mouse model of human brain tumors. NMR in Biomedicine. 2012;25(10):1177-1186.
39. Marin-Valencial, et al. Analysis of Tumor Metabolism Reveals Mitochondrial Glucose Oxidation in Genetically Diverse Human Glioblastomas in the Mouse Brain *In vivo*. Cell Metabolism. 2012;15(6):827-837.